Proceedings of the International Congress on Ultrasonics, Vienna, April 9-13, 2007, Paper ID 1164, Session R12: High power ultrasonic processing
doi:10.3728/ICUltrasonics.2007.Vienna.1164_olikh

Dynamic ultrasound effects in silicon solar cell

Oleg Ya. Olikh, Roman M. Burbelo, Mark K. Hinders[1]

Faculty of Physics, Taras Shevchenko Kyiv National University, Kyiv, Ukraine, olikh@univ.kiev.ua
[1] Applied Science Faculty, The College of William & Mary, Williamsburg, VA, USA

Abstract: The experimental investigation of dynamic MHz ultrasound effect on short current, open circuit voltage, maximal output power and shunting resistance of silicon solar cells have been carried out. The ultrasound intensity is up to 3 W/cm^2. It is revealed that acousto-induced variations of measured parameters depend non-linearly on applied ultrasound intensity and may reach dozens of percents. The analysis of observed effects has been done in an assumption that tunnelling is the prevailing mechanism of carriers drift through the energy barrier.

Key words: Acousto-defect interaction, dynamic ultrasound effect, silicon, solar cell.

A. Introduction

It is known that controllable influence on defective structure of semiconductor devices makes it possible to correct purposefully their characteristics. Nowadays much attention is paid to interaction between ultrasound (*US*) and a semiconductor's defective subsystem [1]-[4]. For example, it is revealed that point defects diffuse in an acoustic field [1]; the radiating defects anneal under *US* action [2], [3]. At the same time the majority of papers are devoted to study of changes of semiconductor properties after *US* treatment while the processes of ultrasonic wave distribution, which are enough interesting [4], are investigated weakly. Our paper represents the results of a dynamic studying (*in situ*) of ultrasound influence on parameters of a silicon solar cell (*SC*).

B. Experiment details

The measured solar cells consisted of a 300-μm-thick *p*-type boron doped silicon substrate (hole concentration is 1.3·10^{15} cm^{-3}) on which surface a 0.5-μm-thick n-Si layer was formed by implantation of P ions ($d_n = 0.5$ μm thick, electron concentration is 10^{19} cm^{-3}). Aluminium contacts were formed on the cell's surfaces: solid contact – on the p-region and semitransparent one – on the n-region.

The current-voltage (*I-V*) characteristics of solar cell was measured both in darkness and under monochromatic illumination. The illumination wavelength were 900 nm or 600 nm. From *I-V* characteristics, measured under illumination, a number of *SC* parameters have been determined, including short current I_{SC}, open-circuit voltage V_{OC} and maximal output power P_M. From dark *I-V*-characteristics the shunt resistance R_{SH} has been determined. *I-V* measurements were carried out during *US* loading too. The ultrasound frequency f_{US} was assigned by resonant modes of the $LiNbO_3$ transducers and was equal 4.1 MHz and 13.6 MHz. Ultrasound induced intensity W_{US} depends on the amplitude of *RF* voltage (U_{RF}), applied to transducer, and reaches up to 3 W/cm^2. A sound waveguide, which consists of a metallic (served for piezoelectric field shielding) and dielectric interlayers, is placed between the transducer and the semiconductor structure. The scheme of the sample arrangement is shown on Fig.1.

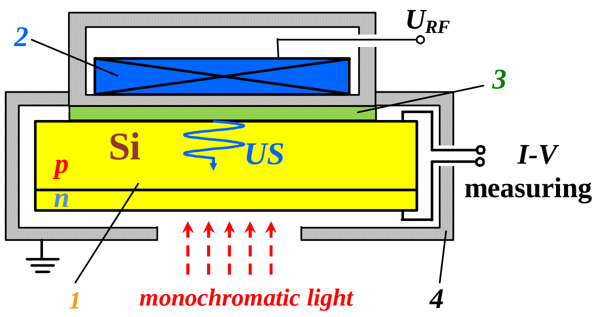

Fig.1. The scheme of an experimental cell. 1 – solar sell; 2 – piezoelectric transducers, 3 – dielectric layer, 4 – electric shield.

In order to separate the elastic vibrations influence on *SC* parameters from the heating effects occurring during ultrasound loading of a sample, measurements of temperature dependences of the investigated parameters were carried out from beginning. It was established, that if temperature increased from room temperature to 350 K, V_{OC} and P_M decreased linearly; while in the same temperature range I_{SC} increased linearly for $\lambda = 900$ nm and remained approximately constant for $\lambda = 600$ nm. We monitored the *SC* temperature during ultrasound action and this allowed us to calculate the expected parameters value, caused by such heating. The difference between the measured *US*-loaded values and the values calculated for a certain *SC* temperature was considered as acousto-induced variation. An example of such dependences is shown in Fig. 2.

C. Experimental results and discussion

At T=295 K and ultrasonic absence, V_{OC}, P_M and I_{SC} values were equal to 210 mV, 1.75×10^{-5} W and 225 μA, respectively, for $\lambda = 900$ nm and 45 mV, 3×10^{-7} W and 25μA for $\lambda = 600$ nm. If solar cell undergone *US* action than these parameters' values increased in comparison to non-ultrasound values at same temperature – see Fig. 2.

doi:10.3728/ICUltrasonics.2007.Vienna.1164_olikh

Dependences of a relative acousto-induced variations of *SC*'s parameters (reached after 2.5-3 hours of acoustic loading) are shown on Fig. 3. The presented dates allow to allocate some features: i) for same W_{US} the variations of I_{SC} and P_M are more profound for 900 nm illumination (exception for P_M for a small W_{US} values only) while a ultrasonic influence on V_{OC} is more essential for $\lambda = 600$ nm; ii) acousto-induced variations depend nonlinearly on ultrasound intensity: the saturation of V_{OC} and P_M is observed for large W_{US} values while dependence of I_{SC} is characterized by a some (about 1 W/cm^2) threshold and variation of short current is stronger after this threshold excess; besides P_M (W_{US}) dependence is non-monotonous as well for 4.1 MHz as for 13.6 MHz; iii) ultrasound of higher frequencies influences more effectively; iv) time needed for a maximal acoustostimulated variations is dozens of minutes - see Fig. 2; v) values of variations are dozens of percents: 10% for I_{SC}, 25 % for V_{OC} and 30 % for P_M.

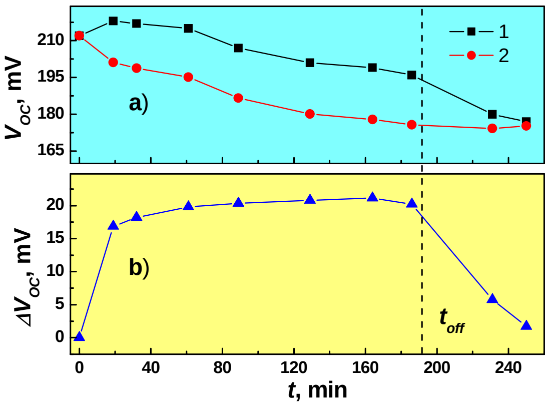

Fig.2. Dependence of V_{OC} versus duration of the ultrasound treatment ($f_{US} = 4.1$ MHz and $W_{US} = 1.5$ W/cm^2). λ = 900 nm. (a): curve 1 shows measured values, curve 2 shows data calculated from temperature dependence, and (b) – difference between these values, the acousto-induced variation of open circuit voltage. The ultrasound loading lasted from $t = 0$ to $t = t_{off}$.

Formfactor K_F is often used for solar sell characterization [5]:

$$K_F = P_M / (V_{OC} I_{SC}) . \tag{1}$$

The dependence K_F on W_{US} has been calculated basing on the experimental data – see Fig. 4. It is evident that dependence's character is different for various wavelengths: for 900 nm K_F increases monotonously with *US* intensity increasing, while for 600 nm the formfactor's recession occurs at low-intensity ultrasound loading.

The approximation of measured forward-biased *I–V* curves was accomplished in accordance with [5]:

$$I(V,T) = I_0 \left[exp(eV/E_T) - 1 \right] + eV/R_{SH} - I_{SC} , \tag{2}$$

where I_0 is saturation currents, E_T is characteristic energy; the last item is absent for the dark *I-V* characteristic. The investigations have shown that the temperature dependence of I_0 can be properly described by the expression $I_0 \sim exp(\chi T)$, where χ is const, while E_T practically remains constant, $E_T = (0.070 \pm 0.003)$ eV. These facts allow concluding that a charge carriers tunneling through the energy barrier is the prevailing drift mechanism in *SC* [5]. In work [6] it is suggested that such tunneling may occur due to charge carriers' transition through a chain of deep levels formed by structural defects in the *p-n* junction region. In this case, *I-V* curves must be described by the equation 2, with E_T characterizing the defects' type.

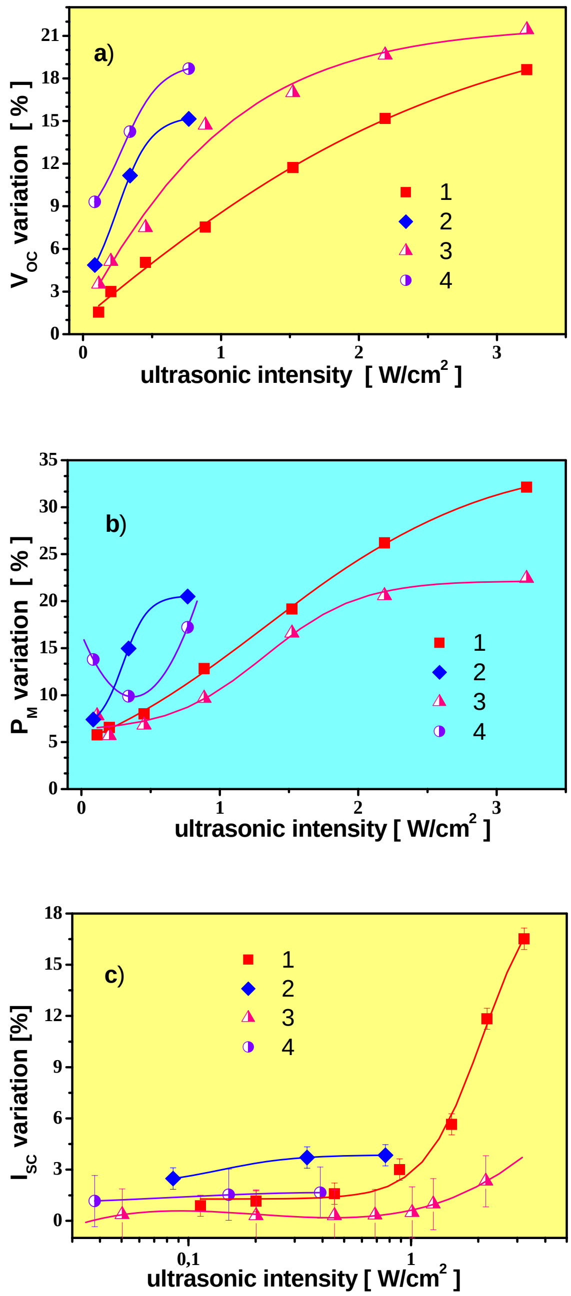

Fig.3. Dependence of relative acousto-induced variations of parameters V_{OC} (a), P_M (b) and I_{SC} (c) on applied ultrasound intensity. The different curves correspond to the different ultrasound frequencies and illumination wavelengths: 1 – $\lambda = 900$ nm, $f_{US} = 4.1$ MHz; 2 – $\lambda = 900$ nm, $f_{US} = 13.6$ MHz; 3 – $\lambda = 600$ nm, $f_{US} = 4.1$ MHz; 4 – $\lambda = 600$ nm, $f_{US} = 13.6$ MHz.

doi:10.3728/ICUltrasonics.2007.Vienna.1164_olikh

The received dependences of ultrasound effect on I_0 and R_{SH} are shown on Fig. 5. The presented dates have shown that the saturation current decreases monotonously and the shun resistance grows practically linearly with W_{US} increase. Besides, it is too evident the greater *US* influence for higher frequency. In our opinion, I_0 reduction is connected with ionization of deep levels located in space charge region and participated in carriers' tunneling. The processes of acousto-induced ionization were observed early [7]. Appearance of R_{SH} is connected often with the processes of current passed through grains boundaries, dislocation and other defects [5]. The acousto-induced ionization of these defects should reduce such currents and, hence, increase R_{SH}.

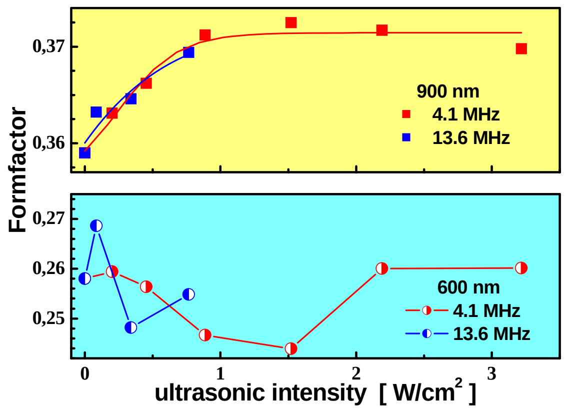

Fig.4. Calculated basing on the experimental data dependencies of solar cell's formfactor for different ultrasound frequencies and illumination wavelengths.

Using (2) one can write down for V_{OC}

$$V_{OC} = (E_T/e)ln[I_{SC}/I_0 - V_{OC}/(I_0 R_{SH}) + 1]. \qquad (4)$$

Current I_{SC} is connected with the photogenerated carriers passed up to the *p-n* junction. The light absorption coefficient α for $\lambda = 600$ nm is equal 4.8×10^3 cm^{-1} and hence it is necessary to consider nonequilibrium carriers, generated both in the *n*-layer and in the vicinity the *p-n* junction (thickness $d_{pn} \approx 0.9$ µm) and inside the *p*-region bulk. Thus

$$I_{SC} = \frac{W_{ph}(1-R)e\beta S_F\lambda}{hc}\{\frac{1-exp(-\alpha d_n)}{1+sd_n/D_p} + \\ +[1-exp(-\alpha d_{pn})]exp(-\alpha d_n) + \frac{\alpha L_n}{1+\alpha L_n}exp(-\alpha(d_n+d_{pn}))\} \qquad ,(5a)$$

where W_{ph} is intensity of the illumination light, R is reflection coefficient, β — quantum efficiency coefficient, S_F — light-absorbing area, L_n — diffusion length of electrons in the *p* region; *s* is surface recombination rate, and D_p — holes' diffusion coefficient inside the *n* region. For λ = 900 nm $\alpha = 0.4\times10^3$ cm^{-1} and in this case it is possible to consider photo-carriers' generation inside the *p*- region bulk only:

$$I_{SC} = \frac{W_{ph}(1-R)e\beta S_F\lambda}{hc}\frac{\alpha L_n}{1+\alpha L_n}. \qquad (5b)$$

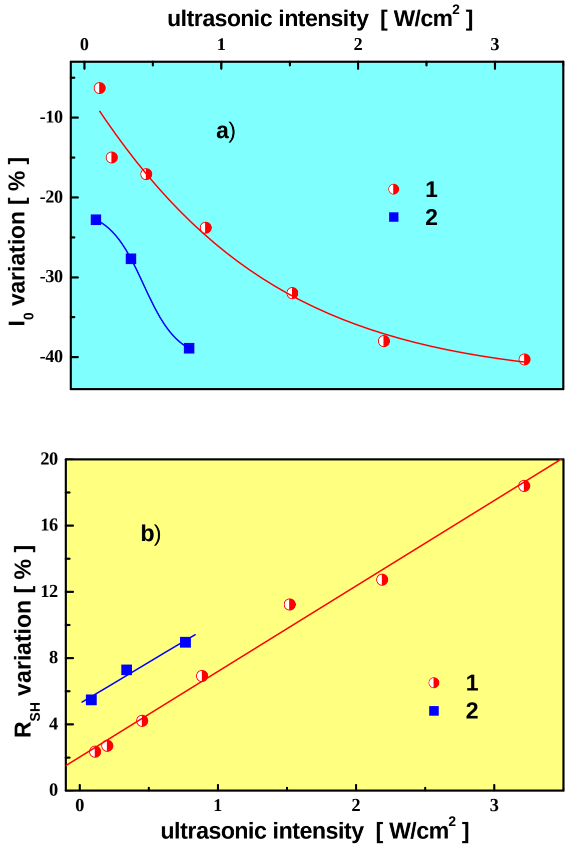

Fig.5. Dependence of relative acousto-induced variations of the solar cell's saturation current (a) and shunt resistance (b) on ultrasound intensity. 1 – $f_{US} = 4.1$ MHz, 2 – $f_{US} = 13.6$ MHz.

One can write for P_M [5]:

$$P_M \approx \frac{E_T}{e}\frac{I_{SC}^2}{(4I_0 + 2I_{SC})}. \qquad (6)$$

The phenomenon of dynamic increase of L_n induced by ultrasound was observed in [8]. According to [8] this phenomenon is connected with reorientation of the complexes of defects induced by the impurity atoms. In our opinion, similar processes are responsible for the observed I_{SC} increase in the case of 900 nm illumination. At the same time, our measurements have shown that $L_n \approx 120$ µm for the solar cell under investigation, hence, $L_n\alpha >> 1$ for $\lambda = 600$ nm and I_{SC} did not practically depend on L_n. In our opinion, it is a reason for much smaller ultrasound effect on I_{SC} for the 600 nm illumination – see Fig. 3(c). The open circuit voltage depends essentially on both I_{SC} and I_0 and R_{SH} – see (4). Thus, for this parameter the processes of defects ionization in the vicinity *p-n* junction are also impotent. Hence, it is necessary to expect a more significant ultrasonic influence in the case of generation of additional carriers in this area. And it is observed on experiment – curves 3 and 4 on Fig. 3(a) pass above the curves 1 and 2, respectively. In our case $I_{SC}/I_0 \approx 50$ for $\lambda = 900$ nm and $I_{SC}/I_0 \approx 5$ for $\lambda = 600$ nm. Thus, according to (6), P_M depends on a photocurrent more essentially than on saturation current; and it is not

doi:10.3728/ICUltrasonics.2007.Vienna.1164_olikh

surprise that dependence of maximal output power's acousto-induced variation on the position of carriers generation is likely to short current's dependence.

D. Conclusion

In this work the experimental investigation of influence of dynamic ultrasound loading on silicon solar cell parameters is made. It is shown that under ultrasound wave action values of short current, open-circuit voltage and maximal output power increase up to dozens of percents. Features of acousto-induced influence are established. In particular, it is shown a growth of influence efficiency with ultrasound frequency increase and effect's dependence on the position of photocarriers generation. The observed effects' features can be explained by acoustic ionization of defects in the vicinity the *p-n* junction and by impurity complexes reorientation inside diode base depth.

E. Aknowledgements

The research was supported by Science and Technology Center in Ukraine (project # 3555).

F. Literature

[1] E. B. Zaveryukhina, N. N. Zaveryukhina, L. N. Lezilova, B. N. Zaveryukhin, V. V. Volodarskii, R. A. Muminov, "Acoustostimulated expansion of the short-wavelength sensitivity range of AlGaAs/GaAs Solar cells," Tech. Phys. Let., vol. 31, pp. 27-32, 2005.

[2] A. A. Podolyan and V. I. Khivrich, " Room-temperature ultrasonic annealing of radiation defects in silicon," Tech. Phys. Let., vol. 31, pp. 408-410, 2005.

[3] Ya. M. Olikh, M. D. Tymochko and A. P. Dolgolenko, " Acoustic-wave-stimulated transformations of radiation defects in γ-irradiated *n*-type silicon crystals," Tech. Phys. Let., vol. 32, pp. 586-58932, 2006.

[4] B. Romanjuk, V. Kladko, V. Melnik, V. Popov, V. Yukhymchuk, A. Gudymenko, Ya. Olikh, G. Weidner, D. Kruger, "Enhanced relaxation of SiGe layers by He implantation supported by in suti ultrasonic treatments," Mat. Sci. in Semicon. Proc., vol. 8, pp.171-175, 2005

[5] A. L. Fahrenbruch and R. H. Bube, "Fundamentals of Solar Cells", New York: Academic, pp. 10-278, 1983.

[6] V. V. Evstropov, M. Dzhumaeva, Yu. V. Zhilyaev, N. Nazarov, A. A. Sitnikova\and L.M. Fedorov, "The dislocation origin and model of excess tunnel current in GaP *p-n* structures", Semiconductors, vol. 34, pp. 1305-1310, 2000.

[7] O. A. Korotchenkov and H. G. Grimmliss, "Long-wavelenght acoustic-mode enhanced electron emission from Se and Te donors in silicon," Phys.Rev.B., vol. 52, pp. 14598-14606, 1995.

[8] O. Ya. Olikh and I. V. Ostrovskii, " Ultrasound-stimulated increase in the electron diffusion length in *p*-Si crystals," Phys. of Sol. State, vol.44, pp. 1249-1253, 2002.